

A NEW SYNCHRONIZED MINIATURE RUBIDIUM OSCILLATOR WITH AN AUTO-ADAPTIVE DISCIPLINING FILTER

Pascal Rochat and Bernard Leuenberger
Temex Neuchâtel Time SA, Switzerland

Abstract

A new rubidium line (SRO) integrating timing functions and time interval measurements was developed using an auto-adaptive disciplining algorithm. This led to an ultra-stable time & frequency machine usable for many applications such as: synchronization of telecommunications systems (SDH, SONET, CDMA), military communications, navigation, and instrumentation.

The frequency and phase-time correction is calculated from an internal phase-time error signal measured within 1 ns resolution issued from an internal PPS signal (PPSINT) aligned to the PPS reference signal (PPSREF). Furthermore, the SRO itself analyzes the stability of the PPSREF signal. Thanks to the very good mid-term frequency stability offered by the rubidium technology. The PPS reference of a GPS engine can be directly applied to the SRO without specific analysis of the internal parameters of the engine (number of satellites in view, signal-to-noise ratio, etc.).

When the "track" mode is selected, the PPSINT is aligned to the PPSREF. Then mid-term frequency stability analysis of the PPSREF (learning phase) may start providing an internal crystal oscillator locked to the rubidium atomic resonance. Such analysis is performed continuously and the PPSINT will then be phase-locked to the PPSREF as long as the Allan variance of the PPSREF is lower than a pre-defined value stored in EEPROM memory. The phase-lock loop time constant t is automatically selected as a function of PPSREF short-term stability. When a standard GPS receiver is used, being affected by selective availability, the typical time constant will be 10,000 to 100,000 sec. Without SA, the typical selected time constant is 1,000 sec.

Details of the principles of the disciplining algorithm are presented as step response and holdover performance data.

THE PRODUCT LINE

Our SRO product line has been designed around two different rubidium cell sizes. The SRO-100 model uses a TNT standard cell size of 14 mm diameter and is able to achieve a very good short-term stability figure as well as a very low drift rate. The SRO-75 is based on the same electronics package, but uses a much smaller Rb cell size. Figure 2 shows the evolution of the size of the rubidium cells (left end: SRO-75; middle: SRO100; right end: LPFRS model).

The SRO models include specific hardware and software for precise phase-time measurement and a phase frequency tracking loop. The time comparison unit consists of a free-running 16-bit counter driven by 7.5 MHz clock signal locked to rubidium atomic resonance. Such atomic resonance is interrogated by a microwave signal issued from the direct multiplication of a 60 MHz signal produced by a third overtone crystal-based oscillator.

Two digital comparators are used to generate external events, such as pulse-per-second signals adjustable in position and width. Furthermore, two additional "time tagging" channels are available for the "time of arrival" of the pulse-per-second reference signal (PPSREF) and an internal pulse-per-

second (PPSINT) generated by the above-mentioned comparators. The main purpose of this internal PPS is to provide a mean of precise time comparisons with the reference signal without having the need to align the output time mark (PPSOUT) to the incoming reference PPS.

Figure 3 shows the complete timing block diagram of the SRO models.

In addition to this system of “time tag” and “time events,” the SRO models include a precise phase-time comparison circuit having a time resolution of 1 ns.

Such a circuit allows precise comparison within ± 500 ns range. This way, the quantification noise added by this circuit is negligible compared to the usual timing noise generated by GPS/PPS signal used as a reference.

DISCIPLINING ALGORITHM

The principal application of a GPS-synchronized fixed communications systems requiring very good “holdover” characteristics is the ability to keep the “time mark” (PPSOUT) within a few microsecond over days. In the same time, ISDN network synchronization requires very good frequency accuracy. Optimal “holdover” performances require a very good estimate of reference frequency in order not to apply wrong frequency corrections to the clock and to be at all times ready for the loss of the incoming reference signal.

In order to achieve optimal performance, TNT designed an adaptive filter that takes into account both the short-term stability of rubidium technology and the long-term stability of the GPS timing signals. Figure 4 shows the typical stability of the SRO with ± 3 °C random temperature variations together with the typical measurement noise generated by the built-in phase-time comparator.

We can see from this graph that the rubidium is always more stable than the time reference combined with the phase comparator for observation times lower than 1000 sec. Therefore, the rubidium line can be used for the estimation of the timing reference stability.

Consider the rubidium typical short-term stability:

$$s_{yRb}(t) = 3 \cdot 10^{-11} \cdot t^{-1/2} \quad \text{for } 1 < t < 1000 \text{ s} \quad (\text{Application Profile I, without temp. deviation})$$

&

$$s_{yRb}(t) = 1 \cdot 10^{-12} \cdot t^0 \quad \text{for } 1 < t < 1000 \text{ s}$$

In case applications with small temperature variations (1°C rms or $\sim \pm 3$ °C) (Application Profile II).

The input time reference is generally affected by white phase-time noise and characterized in the Allan plot by a t^{-1} function (measurement of GPS timing signals with SA or noise added by the internal SRO 1 ns resolution phase-time comparator has demonstrated such characteristics, as shown in Figure 4).

For the Application Profile I without thermal perturbation, the optimal tracking loop time constant t_{loop} is optimized when:

$$s_{yRb}(1s) * t^{-1/2} = s_{yREF}(1s) * t^{-1} \quad (1)$$

For the Application Profile II, with temperature deviations of ~ 1 °C rms, we can consider the short-term stability of the rubidium as limited to:

$$s_{yRbQ}(t) = s_{yREF}(1s) * t^{-1} \quad (2)$$

From Equations 1 & 2, we can then compute the optimal time constant based on the short-term stability of the reference signal compared to the rubidium line for N samples of 1 sec. Furthermore, it is needed to take into account the possible temperature effects in order to switch from one application profile to another. In both cases, the optimal loop time constant is:

Application Profile I:

$$\tau_{loop_opt} = s^2_{yREF}(1s) / s^2_{yRb}(1s) \quad (3)$$

Application Profile II:

$$\tau_{loop_opt} = s_{yREF}(1s) / s_{yRbQ}(t) \quad (4)$$

THE PHASE-FREQUENCY LOOP

The selected phase-time-lock loop filter is based on very standard second-order loop circuit (PI type) characterized by the following equivalent circuit.

The closed loop transfer function of this regulator is expressed by the following:

$$G_{c_s} = K \cdot \frac{\frac{1}{T_i} + s \cdot \frac{T_p}{T_i}}{s^2 + s \cdot K \cdot \frac{T_p}{T_i} + \frac{K}{T_i}} \quad (4)$$

where:

T_i = integrator gain, K = loop gain (1/sec), and T_p = proportional gain.

For a given damping factor z and a given cut-off pulsation w_n of a standard second-order loop control, we can define the T_i and T_p from Equation (4) as follows:

$$T_i = K / w_n^2 \quad (5) \quad \text{and} \quad T_p = 2 * z / w_n \quad (6).$$

THE DISCRETE REGULATOR

The PI regulator shown in Figure 5 has an equivalent discrete circuit diagram.

The two filter coefficients can than be computed using the following relations:

$$K_i = \frac{T_s}{T_i} = \frac{T_s \cdot \omega_n^2}{K} \quad (7)$$

$$K_p = \frac{2 \cdot \zeta}{\omega_n \cdot T_s} - \frac{1}{2} \quad (8)$$

where T_s is filter sampling period. The filter coefficients K_p and K_i can be computed for the Equations (3) & (4) using:

$$\tau_{loop_opt} = 1 / w_n \quad \text{and} \quad T_s \ll \tau_{loop_opt}$$

For Application Profile I, the filter coefficients become:

$$K_i = \frac{T_s \cdot \sigma_{yRb}^4(1)}{\sigma_{yREF}^4(1) \cdot K} \quad \& \quad K_p = \frac{2 \cdot \zeta \cdot \sigma_{yRb}^2(1)}{K \cdot \sigma_{yREF}^2(1)}$$

For Application Profile II (automatically selected; see next section), the two filter coefficients can be computed using the following relations:

$$K_i = \frac{T_s \cdot \sigma_{yRb\theta}^2(1)}{\sigma_{yREF}^2(1) \cdot K} \quad \& \quad K_p = \frac{2 \cdot \zeta \cdot \sigma_{yRb}(1)}{K \cdot \sigma_{yREF}(1)}$$

APPLICATION PROFILE SELECTION

The SRO model is equipped with an internal thermometer and thermal stability is computed using a 100-second time interval. Such temperature stability is then used for an automatic switchover from the first equation calculation method to the second. Such a temperature stability evaluation method needs to be improved and more intensive testing still needs to be done.

AUTO-ADAPTIVE TIME CONSTANT TEST

Figure 9 represents the response of the SRO to a phase-time step of +200 ns. Such a phase step is generated by a synthesizer providing a 10MHz signal synchronized to the maser reference $+10^7$ divider. In addition, the phase of this reference signal can also be modulated with a random or sinusoid waveform. Figure 9 shows clearly automatic time constant adaptation when applying 6 ns rms phase-time noise to the PPSREF signal of the SRO.

HOLDOVER CHARACTERISTICS

The auto-adaptive circuit should help to keep the rubidium as stable as possible. This way, the average reference frequency estimation is improved.

So far the SRO always used a fixed number of points for the calculation of the reference noise standard deviation. Figure 8 shows a typical holdover characteristic. We can clearly see the steps of 133 ns when the precise internal phase comparator is out of the ± 500 ns range.

We can see from this result that the SRO is able to keep its output phase within 1 μ s being driven with a noisy reference signal.

CONCLUSION

The SRO models auto-adaptive algorithm has been successfully tested and some improvements in terms of averaging time, number of samples, and temperature variation estimates are still planned after the complete statistic of performance tests are done on the first 100 production/qualification units.

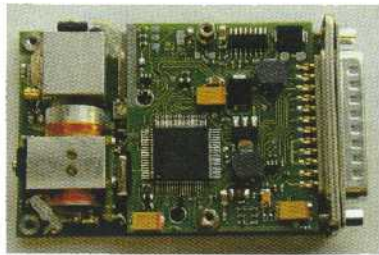


Fig. 1: Inside view of a SRO100.

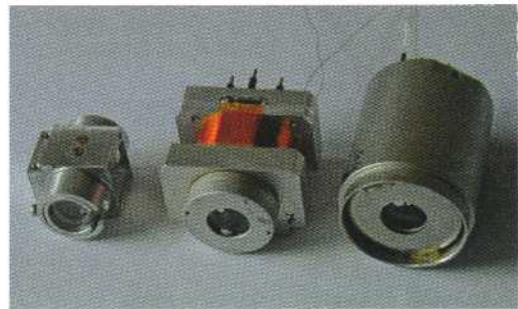


Fig. 2: SRO-75, SRO100, LPFRS Rb cells.

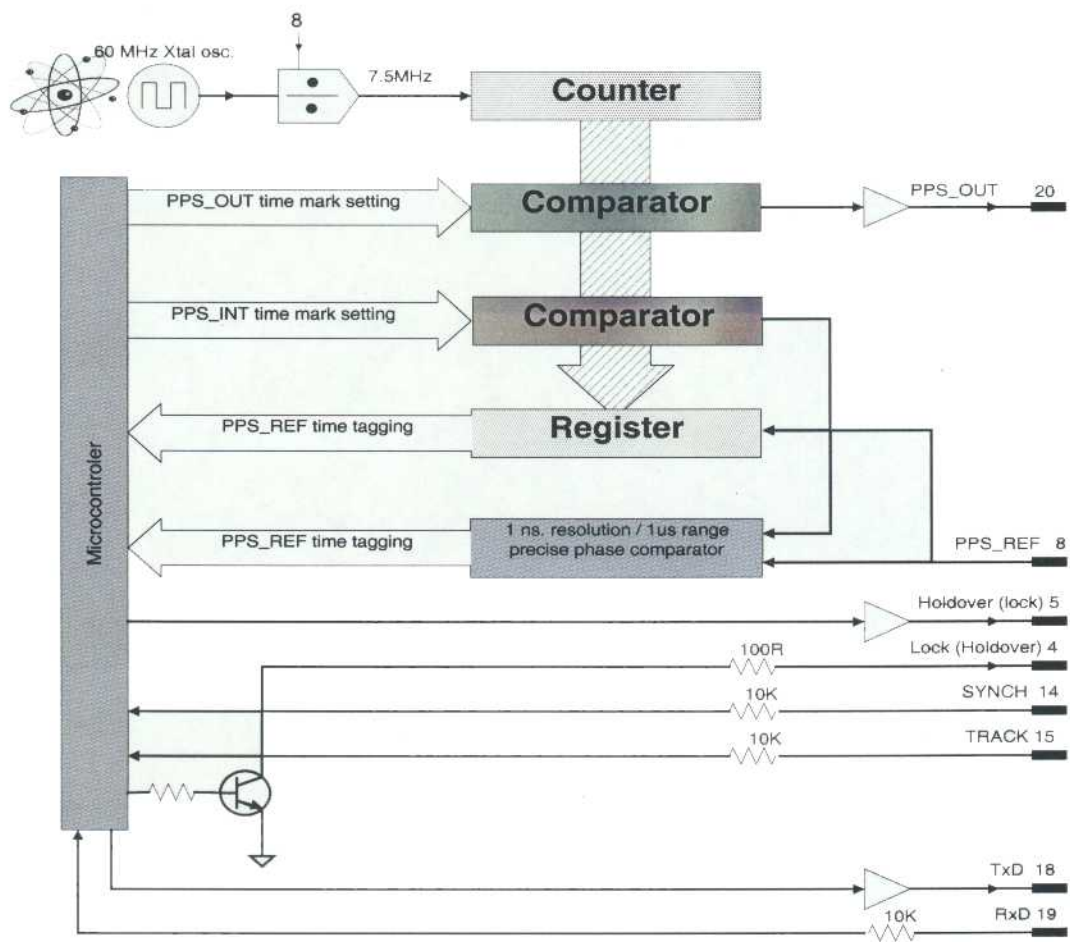


Fig.3: SRO time subsystem block diagram.

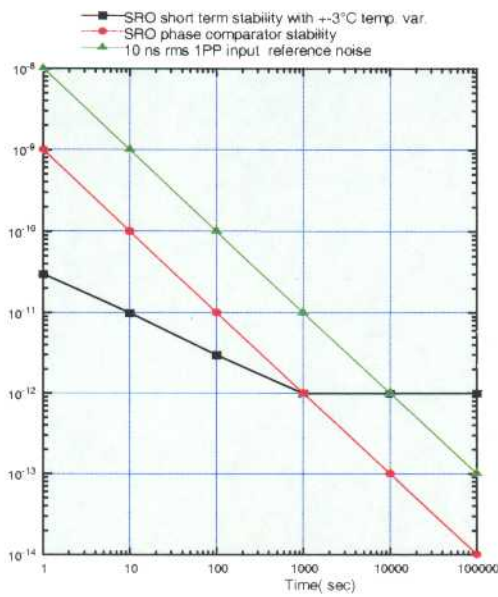


Fig. 4: Typical stability data.

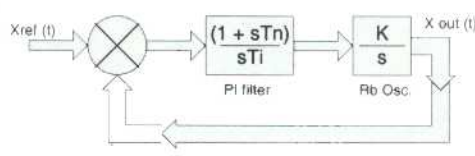


Fig. 5: PI regulator block diagram.

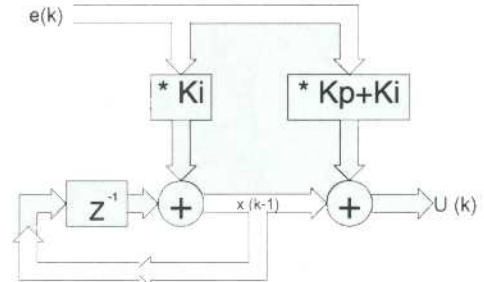


Fig. 6: Discrete PI filter.

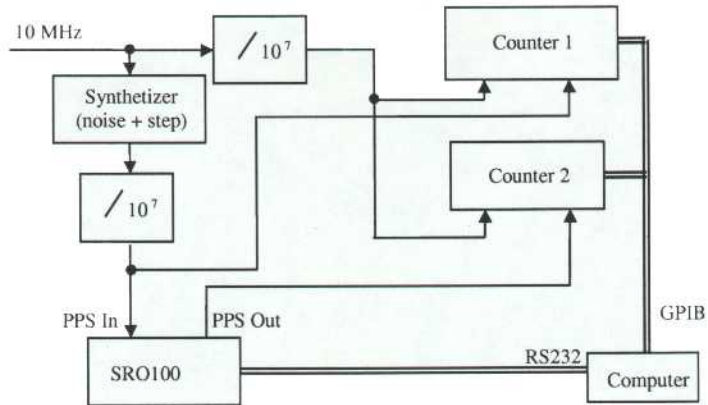


Fig. 8: Measurement setup.

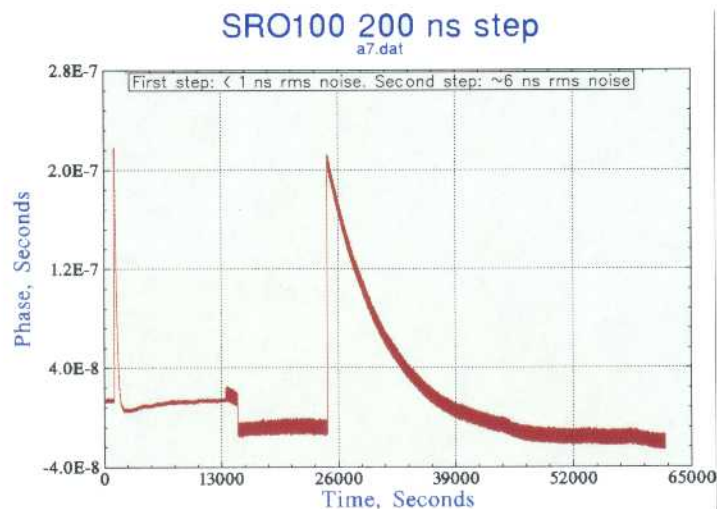


Fig. 9: Step response, with/without PPS Ref noise.

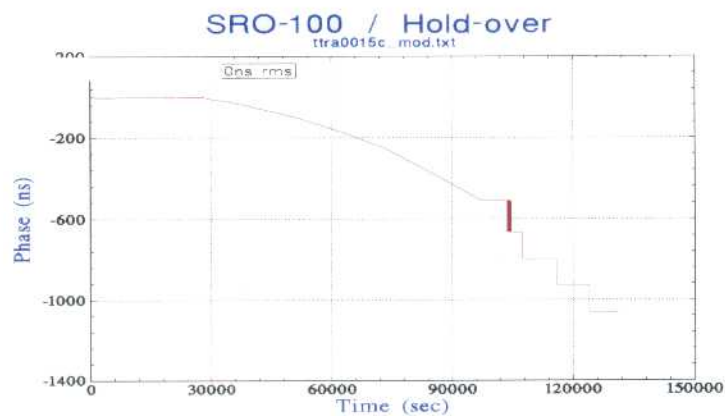


Fig. 8: Holdover plot using SRO phase comparison.